Numerical and experimental exploration of the fundamental nonlinear dynamics of self-centring damage resistant structures under seismic excitation

O. Oddbjornsson, N.A. Alexander & C.A. Taylor
Department of Civil Engineering , University of Bristol, Bristol, UK

R. Sigbjornsson
Department of Civil Engineering, University of Iceland, Reykjavik, Iceland

SUMMARY:
Current elasto-plastic design has succeeded in reducing the number of casualties, during large seismic events, while economic losses have grown significantly. These financial losses have emphasized the need for more elaborate damage resistant structures. These structures are capable of exhibiting large deformations while still remaining elastic (although nonlinear), in contrast with current earthquake resistant structures which go plastic. Precast concrete frames with post tensioned tendons connecting elements are a typical example of this class of structure.
A physical model of the aforementioned class of structure was tested both statically and dynamically. Through nonlinear system identification techniques, a simplified numerical representation of the physical model was generated and then validated against its physical counterpart. The physical and numerical models confirmed the existence of nonlinear dynamic phenomena, such as coexisting solutions over a wide frequency range, as well as sensitivity to harmonic and seismic excitation parameters, within both models.

Keywords: Damage Resistant, Self-Centring, Post-Tension, Excitation Sensitivity, Seismic Excitation

1. INTRODUCTION

Current seismic design codes, such as practised today in USA and Japan, achieve live safety by allowing the structure to go plastic at predefined locations, during large seismic events. This design philosophy has succeeded in reducing the number of casualties, while the economic losses have grown significantly. As an example, the Northridge earthquake in 1994 resulted in only 57 casualties while the economic losses reached $50 billion (Porter et al., 2006). These financial losses, associated with current elasto-plastic ductility design, have shifted the engineering practice towards damage resistant structures. These nonlinear elastic moment resisting frames (NLEMRFs) are capable of exhibiting large deformations while still remaining elastic (although nonlinear), in contrast with current earthquake resistant structures which go plastic. These structures have self-centring capabilities and consequently do not exhibit residual deformations. Furthermore, they can easily take advantage of additional energy dissipation mechanisms without impairing their self-centring capabilities (Dietz, 2010). Consequently, the post-earthquake serviceability of these structures is not impaired.

Precast concrete frames with post tensioned tendons connecting elements are a typical example of this class of structure. They exhibit nonlinear softening stiffness characteristics arising from geometric distortions and tendon tension changes.

Even though NLEMRFs have been researched extensively over the last 15-20 years, the dynamic characteristics of these highly nonlinear structures are still relatively unknown. To date, large numbers of confined beam-column assemblies have been tested under cyclic loading up to failure. In addition to these tests, a 60% scale 5-story, 2-bay model building, employing the NLEMRF concept, tested pseudo-dynamically up to excitation levels 50% beyond the design level by Priestley et al (1999). The evidence gathered from these tests were compelling, with only a minimal amount of damage observed

all the way up to design level.

Although the dynamic properties of this class of structure are largely unknown, vast information on the dynamic response of nonlinear systems exists within the nonlinear dynamics field (Thompson and Stewart, 2002). The existence of complicated nonlinear dynamics has been confirmed for numerous physical problems such as capsize of ships and rocking blocks. These simple nonlinear systems exhibit complicated behaviour such as sensitivity to excitations as well as initial conditions.

This paper examines the potentially complicated dynamic response of this class of structure under a wide range of excitations, with the help of a scaled physical model and a numerical model. The physical model, representing a generic structure of the NLEMRF type, was used to investigate the fundamental characteristics of this class of structure under both static and dynamic loading. The data retrieved during the physical experiments was then used to produce and validate a simplified numerical representation of the physical model. Finally the dynamics of the simplified numerical representation were explored over a wide range of both seismic and harmonic excitations. Techniques from the wider nonlinear dynamics field as well as new analysis techniques, derived from the standard ones, were used to explore the nonlinear dynamics.

2. MODELLING

Prior to the work presented in this paper, a numerical model, employing the distinct element method, was used to identify the existence of typical nonlinear dynamic features within a generic NLEMRF (Oddbjornsson et al., 2007). Nonlinear dynamic phenomena identified within this model include a nonlinear resonance response curve having coexisting solutions over a wide range of excitation frequencies as well as jumps between its two branches. The distinct element method's ability to replicate the dynamic characteristics of a NLEMRF was verified by comparing the response of a scaled physical model to its numerical representation (Oddbjornsson et al., 2008). Although the distinct element method is able adequately to model this class of structure, the analyses are several orders of magnitude too time consuming to be used properly to characterise the nonlinear dynamics.

A reduced scale physical model of a generic NLEMRF allows the nonlinear dynamic features of a real structure, made from real materials with its manufacturing tolerances and other imperfections, to be explored. A physical model can also be used to assess the system's self-centring capabilities as well as whether its characteristics are invariant, e.g. that repeated tests produce the same result. Furthermore, dynamic properties such as damping and response frequency amplitude dependence can be investigated. Finally, a physical model provides a benchmark to produce and validate numerical models against.

Since physical testing is both expensive and time consuming, conducting the large number of physical tests necessary thoroughly to investigate the dynamics of the system is not feasible. When used in parallel with physical experiments, numerical modelling provides an important and efficient way of overcoming some of the problems associated with physical modelling. A single degree of freedom (SDOF) numerical representation of the physical model can be used to explore the system's nonlinear dynamics over a wide range of parameters for both harmonic and stochastic excitations (Alexander et al, 2011).

2.1. Physical Model

Based on a single storey light weight portal frame prototype building, a physical model representing a single bay frame from the prototype at quarter scale was produced (Oddbjornsson, 2009), see Fig. 2.1. The model scaling was done in accordance with the artificial mass simulation scaling rules (Harris and Sabnis, 1999). The model frame had a 2100mm (c/c) bay width and 900mm column height (base to beam centre). A two tonne mass, attached to the top of the frame, represented the scaled seismic inertia mass. The base shear was determined according to the Direct Displacement Based Design

method (Priestley, 2002) for a design drift of 2.5%. The detailed design of the model was done according to provisional design guidelines (Stanton and Nakaki, 2002). Following the design guidelines for an initial joint contact area of 100x100mm, tendon tension force and cross sectional area of 115kN and 93mm^2 for beam tendons and 64kN and 52mm^2 for column tendons were required. The beam and column elements were made from 100x100x10mm square hollow steel tube, having 20mm thick endplates. The joint contact area between elements was steel to steel. The fact that the frame was made from steel rather than concrete does not influence the global behaviour of the system since its characteristics are primarily associated with the properties of joints between elements rather than the elements themselves.

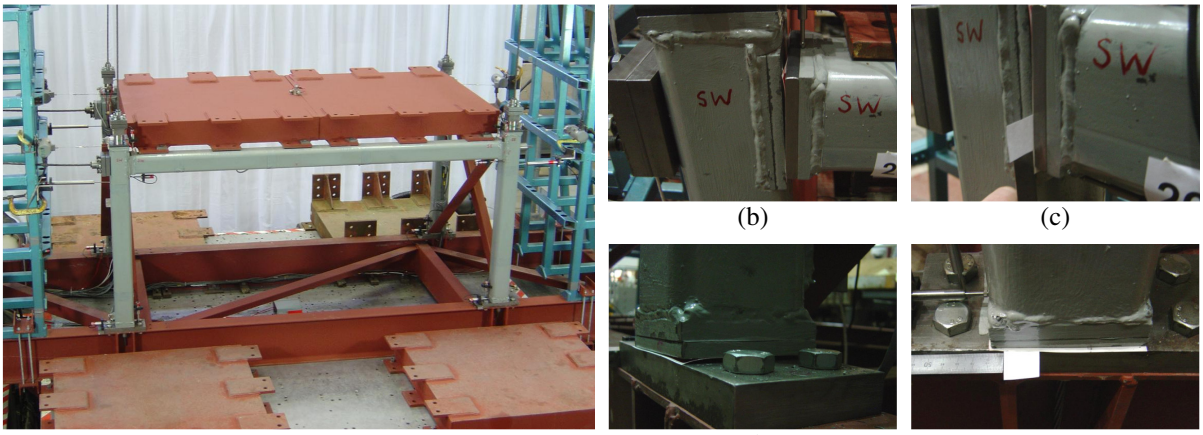

(a) (b) (c) (d) (e)

Figure 2.1. The reduced scale physical model; overview (a), beam-column joint (b), beam-column joint contact depth (c), column-foundation joint (d) and column-foundation joint contact depth (e)

2.2. Simplified Numerical Model

In recent years, the linear least squares method (Hsia, 1977), conventionally used for determining an optimal fit of a set of predefined numerical functions to a data set, has been employed to identify a system's equation of motion (EOM) for nonlinear systems (Nelles, 2001). To produce a realistic model capable of representing the structure over as much of its parameter space as possible, it is important that the data set used for system identification includes as wide a range of response properties as possible. Using the derived numerical model to predict the system's response outside the range of the data set by extrapolation does normally not produce good results. Therefore, to produce the best possible SDOF numerical representation of the physical model, data sets recoded during sine sweep tests were utilized during the nonlinear system identification process. These data sets included the system's characteristics over a wide range of excitation parameters and response amplitudes.

Through trial and error, starting with a complex set of functions, all being integer power combinations of the system's displacement and velocity, an SDOF expression capable of representing the physical model adequately was identified as

$$\ddot{x} + f_d(x,\dot{x}) + f_k(x) = -\ddot{x}_g \tag{2.1}$$

where the damping force f_d is equal to

$$f_d(x,\dot{x}) = a_5\dot{x} + a_6\dot{x}|\dot{x}| + a_7\dot{x}e^{(d_2 x)}\tanh(d_3|x|) + a_8\dot{x}\tanh(d_4|x|) \tag{2.2}$$

and the restoring force f_k is equal to

$$f_k(x) = a_1 x + a_2 x|x| + a_3 x^3|x| + a_4\tanh(d_1 x), \tag{2.3}$$

where a_i and d_i are the unknown parameters to be determined through linear least squares. The d_i

parameters in the equation are within a nonlinear function and therefore can not be identified directly through linear least squares. To resolve this issue, rather than employing computationally inefficient nonlinear least squares, linear least squares was conducted in a loop, assessing the error while varying each d_i from an initial vector **d**, to find a local minimum (Oddbjornsson, 2009). The a_i and d_i values for Eqn. 2.1, identified in the aforementioned way, can be found in Table 2.1 below.

Table 2.1. Coefficients of the EOM determined through nonlinear system identification

a_1	a_2	a_3	a_4	a_5	a_6	A_7	A_8	d_1	d_2	d_3	d_4
-1570.3	5.661e4	-1.937e7	29.63	6.95	-6.09	48.27	-28.81	149.00	-23.50	77.00	129.00

3. FUNDAMETAL MECHANICS

Before investigating the dynamic response characteristics of this class of structure under base excitation, it is important to understand their fundamental mechanics by conducting simple replicable tests. Furthermore, the data gathered through those tests can be used to investigate the validity of the SDOF EOM presented in section 2.2.

The fundamental mechanics of the reduced scale physical model were investigated using a series of pushover, pull-back and free vibration (snapback) tests. The model's nonlinear force-deflection characteristics for both positive and negative sway were confirmed by pushover and pull-back tests, see Fig 3.1 (a). Data from repeat tests fell on the same line, confirming the elasticity and the consistency of the response. The model's dynamic properties were investigated through free vibration tests. By taking the time between zero crossings, during free vibration tests, the model's amplitude dependant response frequency associated with its nonlinear softening stiffness characteristics was confirmed. The free vibration data was also used to estimate the model's equivalent viscous damping and how it is related to the response amplitude. An average damping ratio over 3 response cycles was calculated through standard logarithmic decrements as a running average and plotted against the average peak response amplitude over the 3 response cycles, see Fig. 3.1 (b). Furthermore, the level of joint opening and joint shear movements were monitored and compared against assumptions made by the design codes.

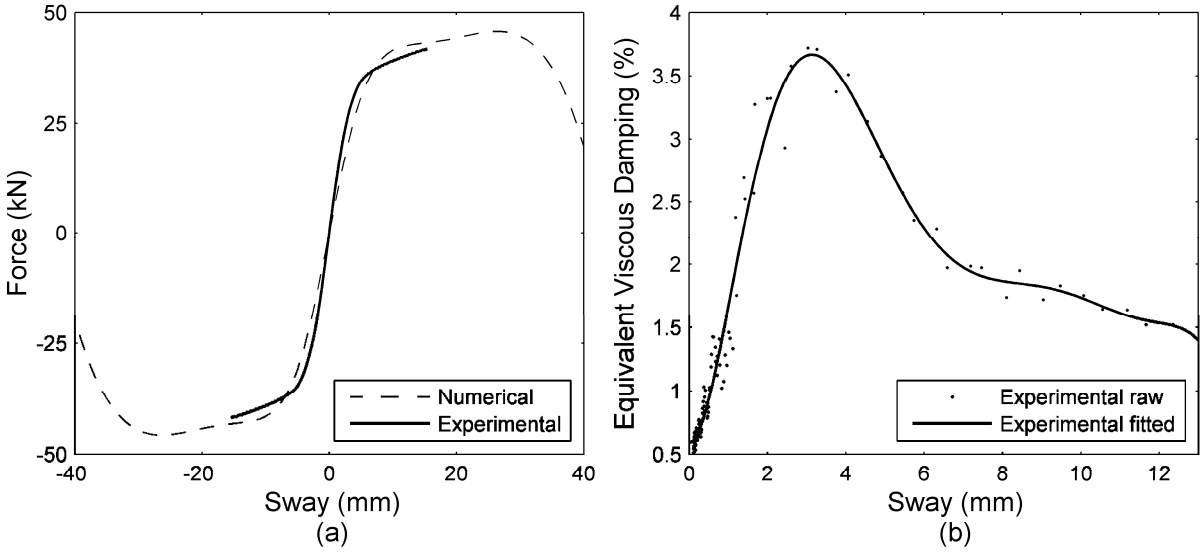

Figure 3.1. Pushover curves for both physical and numerical models (a) and equivalent viscous damping characteristics of the physical model (b)

The stiffness and damping characteristics of the SDOF numerical representation were compared against its physical model's counterparts. The restoring force f_k, is plotted alongside the physical model's quasi-static force-deflection curve, showing very similar characteristics, see Fig. 3.1 (a). Although the fit between the physical model's quasi-static force-deflection curve and the numerical

model's restoring force characteristics is good overall, the numerical model is initially marginally softer and then at higher amplitude response it produces somewhat higher restoring forces. It is, though, worth noting that the numerical model's force-deflection characteristics are derived from dynamic data while the physical model's curve is quasi-static. A comparison of the damping properties are somewhat more difficult to achieve since the SDOF model's damping is dependent on both displacement and velocity. By assuming that the damping takes the form of conventional mass proportional Rayleigh damping, it is possible to derive an expression of the instantaneous equivalent viscous damping as a function of displacement and velocity (Oddbjornsson, 2009). This expression takes the form

$$\zeta_n(x,\dot{x}) = \frac{a_5 + a_6|\dot{x}| + a_7 e^{(d_2 x)} \tanh(d_3|x|) + a_8 \tanh(d_4|x|)}{2\sqrt{a_1 x + a_2 x|x| + a_3 x^3|x| + a_4 \tanh(d_1 x)}}, \tag{3.1}$$

where ζ_n is the instantaneous equivalent viscous damping ratio. A graph depicting this expression is produced for every realistic spatial coordinate, see Fig. 3.2 (a). Qualitative comparison between Fig. 3.1 (b) and Fig. 3.2 (a) reveals similar behaviour with intermediate level response producing the largest amount of damping with higher and lower level responses having less damping. Finally, the sum of the damping force f_d and the restoring force f_k is presented as a function of the spatial coordinates, see Fig. 3.2 (b).

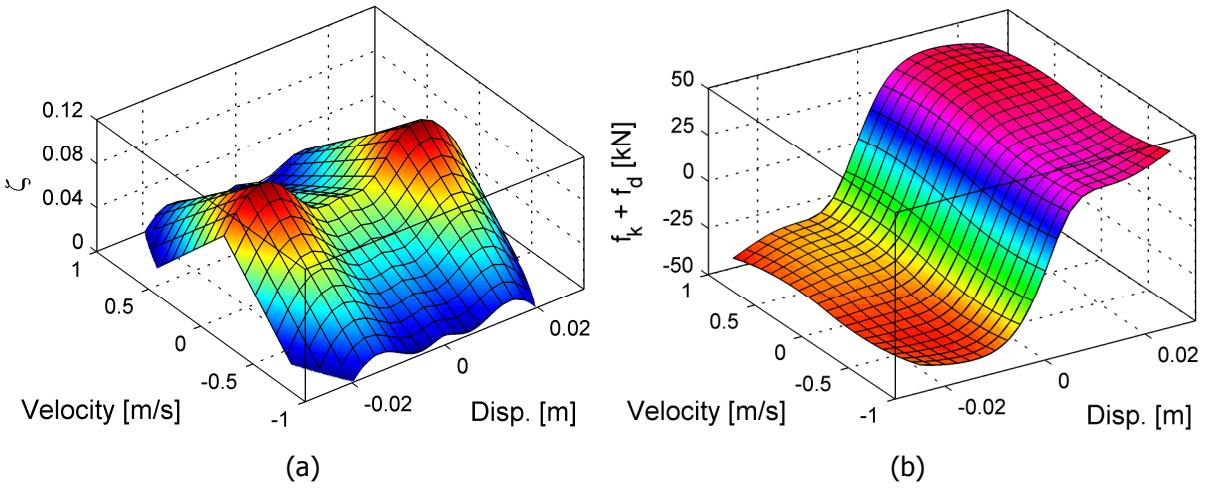

Figure 3.2. The SDOF numerical model's equivalent viscous damping (a) and sum of the damping and restoring force (b) with respect to spatial coordinate

This study has demonstrated the fundamental mechanics of both the physical model and the SDOF numerical model. A comparison of the two has confirmed that the SDOF numerical model is a good representation of its physical counterpart, at least in relation to the fundamental mechanics.

4. NONLINEAR DYNAMICS UNDER HARMONIC EXCITATION

With the fundamental mechanics of the system understood, the next step is to look at the response under dynamic excitation. The simplest type of dynamic excitation, harmonic excitation, allows the nonlinear dynamic characteristics of the models to be investigated with the help of standard tools from the nonlinear dynamics mathematics field. For both the SDOF numerical and the physical model, increasing and decreasing frequency sine-sweep tests were conducted to explore their nonlinear resonance response curves. A comparison between the sine-sweep test results for the SDOF numerical and the physical models is presented in Fig 4.1 (a) and (b) for low level excitation (0.10g) and high level excitation (0.26g) respectively. Qualitatively, there is a good agreement between the SDOF numerical and the physical models. At high level excitation, both the shape and the response

amplitudes are very similar for both models, with two coexisting solution existing over a wide frequency range. At low level excitation, although the shape is quite similar, the numerical model is somewhat softer than the physical model resulting in higher amplitude response and lower resonance frequency. It is worth noting that the shaking table control was far from perfect, particularly when the structure exhibited large amplitude response, which could explain some of the differences between the two model responses. Overall, the SDOF numerical model is able to capture the resonance response characteristics of the physical model reasonably well.

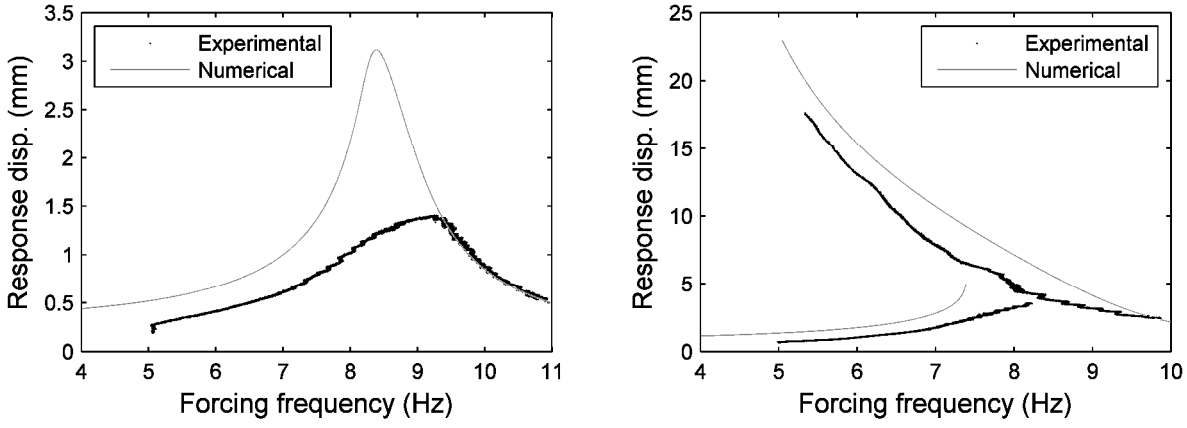

Figure 4.1. Comparison between the resonance response curves of the physical and numerical models at low (0.10g) (a) and high (0.26g) (b) excitation amplitudes

Since the numerical model is able to adequately represent both the physical model's fundamental mechanics and resonance response characteristics, it is possible to use it to explore the physical model's dynamics over a much wider range. From a practical point of view, the numerical model is normalized with respect to its low amplitude (linear) response frequency and design strength. Using a standard analysis technique, harmonic excitation control space diagrams, it is evaluated how many harmonic forcing cycles it takes the system to reach failure, see Fig 4.2 (a) and (b) for the global overview and the first sub-harmonic respectively. The control space diagrams demonstrate the system's sensitivity to excitation parameters, with the system exhibiting failure at particular excitation amplitude while not failing at a higher one. Areas where two excitation parameters very close together produce vastly different results are observed, particularly around the first sub-harmonic.

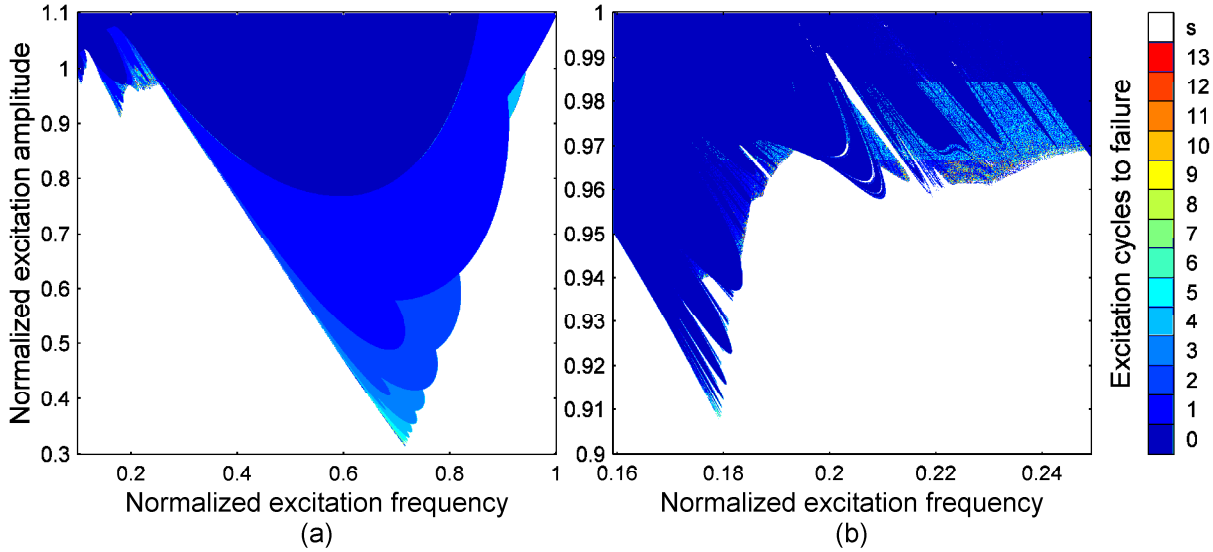

Figure 4.2. Harmonic excitation control space diagrams, overview (a) and at and above the first sub-harmonic (b)

5. NONLINEAR DYNAMICS UNDER SEISMIC EXCITATION

In section 4, the existence of nonlinear dynamic phenomena such as two stable solutions over a wide frequency range (using both physical and numerical models) and sensitivity to excitation parameters (only for numerical model) was demonstrated. Now the questions are if and how these nonlinear dynamic phenomena will manifest them self under seismic excitation.

Traditionally, incremental dynamic analysis is used to explore the sensitivity of a model to seismic excitation. In incremental dynamic analysis the earthquake excitation is applied to the model at increasing amplitudes, by scaling the amplitude of the earthquake as a whole, and the response compared to the earthquake amplitude. To demonstrate that both the physical and numerical models exhibited comparable characteristics under seismic excitation, incremental dynamic analysis were conducted, see Fig 5.1 (a) and (b) for the Loma Prieta and Northridge earthquakes respectively. Fig 5.1 relates the model's peak response displacement to the earthquake's peak ground acceleration (PGA). The sudden change in gradient of the peak response to PGA indicates a shift from the low amplitude attractor to the high amplitude attractor in the coexisting solution frequency range. A good agreement is observed between the numerical and physical model results, further confirming the validity of the SDOF numerical model.

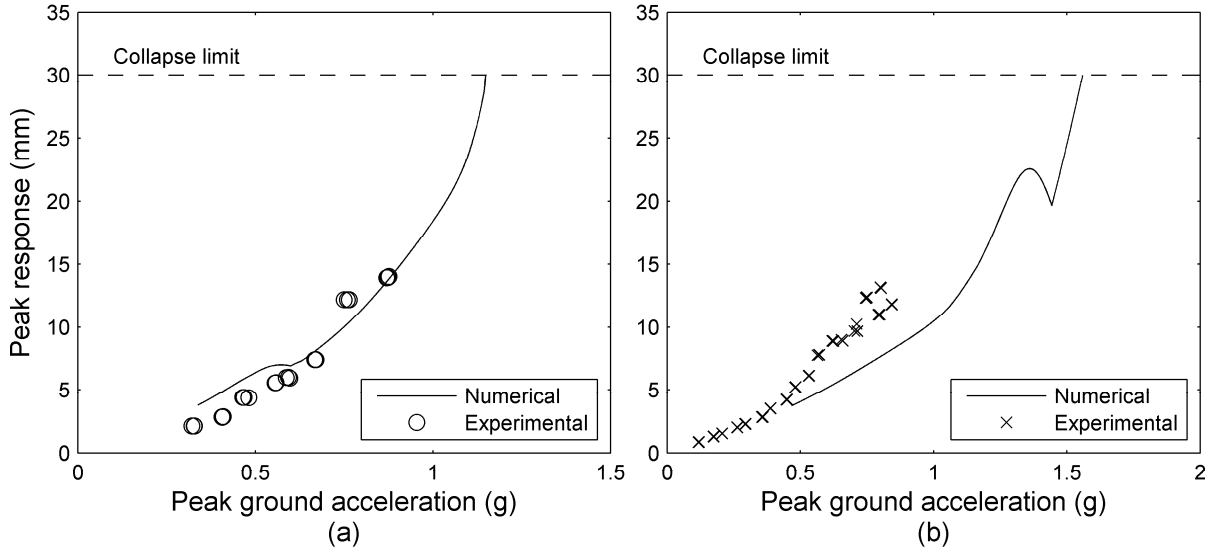

Figure 5.1. Incremental dynamic analysis for the Loma Prieta Earthquake (a) and the Northridge Earthquke (b)

Finally, a new analysis method, able to explore the sensitivity to seismic excitation's frequency and amplitude content, is presented (Oddbjornsson, 2009). This method, an addition to the incremental dynamic method, explores a system's response to a seismic time history scaled as a whole both in frequency and amplitude. This new method is used to produce seismic excitation control space diagrams using the SDOF numerical model, see Fig. 5.2 (a) and (b) for the Loma Prieta and Northridge earthquakes respectively. In these graphs, the x and y axis represent the earthquake's overall frequency and amplitude scales respectively (where coordinate 1,1 denotes the original earthquake), with the model's peak response amplitude represented by the colour. These seismic control space diagrams demonstrate how sensitive the system is to variation of the seismic excitation, with a small change in the earthquake's overall frequency or amplitude having dramatic influence on the model's response. Areas where a small change in the earthquake's frequency or amplitude separates between moderate response and collapse are identified for both earthquakes, indicating a shift from the lower amplitude branch to the higher amplitude branch of the resonance response curve.

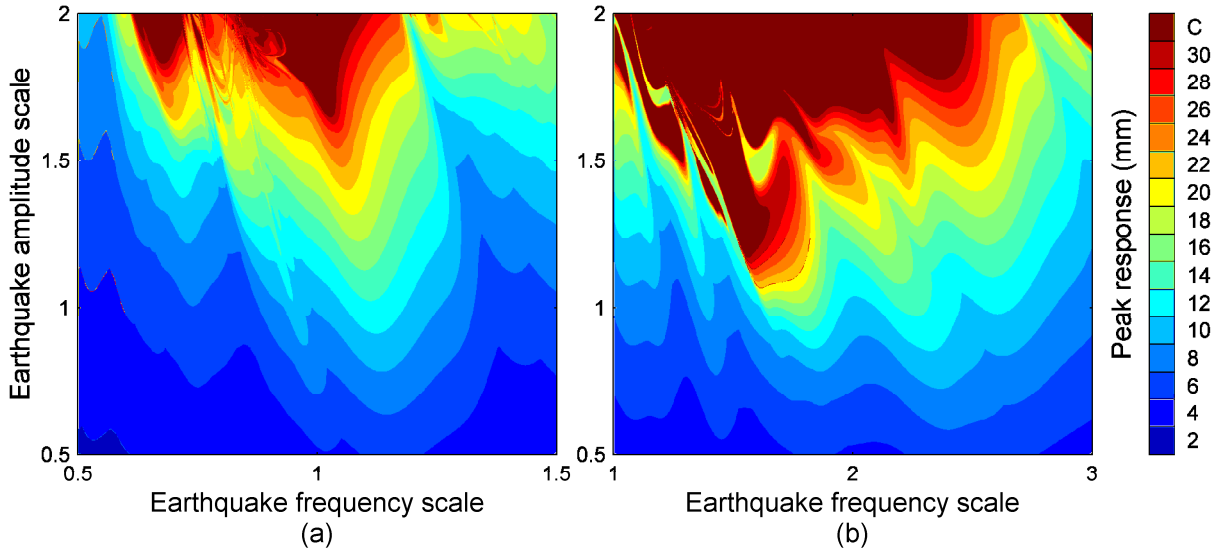

Figure 5.2. Seismic control space diagrams for the Loma Prieta Earthquake (a) and the Northridge Earthquke (b)

6. CONCLUSIONS

A reduced scale physical model, representing a building from a new class of damage resilient structures, was tested both statically and dynamically. Using nonlinear system identification techniques, the data gathered during physical model testing was used to produce a SDOF numerical representation. Through simple tests, the fundamental mechanics of both the physical and SDOF numerical models weree investigated. Finally, the nonlinear dynamic characteristics of both models were explored for both harmonic and seismic excitations.

Through quasi-static pushover (pull-back) tests, the physical model's nonlinear softening stiffness characteristics were confirmed. A comparison between the physical model's and the SDOF numerical model's stiffness curves demonstrated that the SDOF numerical model was able to capture the physical model's stiffness characteristics. Free vibration (snap-back) tests were used to explore the damping characteristics of the physical model. It was revealed that the equivalent viscous damping characteristics of the physical model were qualitatively the same as its numerical counterpart's.

Increasing and decreasing frequency sine-sweep tests were used to identify the physical and numerical model's nonlinear resonance response curves. For both models, co-existing solutions were identified over a wide frequency range with jumps between the two branches. A good agreement between the numerical and physical model results was observed. Harmonic excitation control space diagrams were produced for the SDOF numerical model. These diagrams revealed the system's sensitivity to harmonic excitation parameters.

To validate the numerical model against the physical model for seismic excitation, incremental dynamic analyses were conducted, employing the Loma Prieta and Northridge earthquakes. These tests demonstrated that the numerical model was able adequately to represent the physical model for seismic excitation. A new method, an addition to the incremental dynamic method, able to explore system's sensitivity to earthquake's amplitude and frequency content is presented. Using this new method, seismic excitation control space diagrams are produced for the Loma Prieta and Northridge earthquakes. These diagrams demonstrate the model's sensitivity to seismic excitation, with a small deviation in the earthquake's frequency or amplitude content separating between moderate response and collapse.

AKCNOWLEDGEMENT
The researchers would like to thank Carrington Wire and CCL Stressing Systems for supplying the high strength

steel strands and the cable grips needed to conduct this research free of charge. Furthermore, we would also like to acknowledge that Rannis, The Icelandic Centre for Research, and Landsvirkjun, The Icelandic National Power Company, supported Olafur Oddbjornsson financially to conduct this research as a part of his PhD study.

REFERENCES

Alexander, N.A., Oddbjornsson, O., Taylor, C.A., Osinga, H.M. and Kelly, D.E. (2011). Exploring the dynamics of a class of post-tensioned, moment resisting frames. *Journal of Sound and Vibration*. 330:15, 3710-3728.

Dietz M., Oddbjornsson O., Taylor C.A., Ojaghi M., Williams M.S., Blakeborough A. (2010). Shaking table testing of a post-tensioned tendon frame retrofitted with metallic shear panel dissipator. *9th US/10th Canadian Conference on Earthquake Engineering*. Paper 1185.

Harris, H.G. and Sabnis, G.M. (1999). Structural modeling and experimental techniques, CRC Press, Boca Raton, Florida, U.S.A.

Hsia, T.C. (1977). System identification : least-squares methods, Lexington Books, Lexington, Mass.

Nelles, O. (2001). Nonlinear system identification : from classical approaches to neural networks and fuzzy models, Springer, Berlin ; New York, U.S.A.

Oddbjornsson, O. (2009). Dynamics of nonlinear elastic moment resisting frames, Univeristy of Bristol, Bristol.

Oddbjornsson, O., Alexander, N.A., Taylor, C.A. and Sigbjornsson, R. (2007). Computational Analysis of Precast Concrete Frames with Post-Tensioned Tendons. *Proceedings of the Eleventh International Conference on Civil, Structural and Environmental Engineering Computing*. Paper 167.

Oddbjornsson, O., Alexander, N.A., Taylor, C.A. and Sigbjornsson, R. (2008). Shaking Table Testing of Nonlinear Elastic Moment Resisting Frames. *14th World Conference on Earthquake Engineering*. Paper 11-0110.

Porter, K., Shoaf, K. and Seligson, H. (2006). Value of injuries in the Northridge earthquake. *Earthquake Spectra.* **22:2**, 555-563.

Priestley, M.J.N. (2002). Direct displacement-based design of precast/prestressed concrete buildings. *Pci Journal.* **47:6**, 66-79.

Priestley, M.J.N., Sritharan, ., Conley, J.R. and Pampanin, S. (1999). Preliminary results and conclusions from the PRESSS five-story precast concrete test building. *Pci Journal.* **44:6**, 42-67.

Stanton, J. and Nakaki, S. (2002). Precast Seismic Structural Systems PRESSS Vol. 3-09: Design guidelines for precast concrete seismic structural systems, University of Washington, Seattle, U.S.A.

Thompson, J.M.T. and Stewart, H.B. (2002). Nonlinear dynamics and chaos, John Wiley, Chichester, U.K.